Nature of the First Electron Transfer in Electrochemical Ammonia Activation in a Nonaqueous Medium

Citation: Schiffer, Zachary et al. "Nature of the First Electron Transfer in Electrochemical Ammonia Activation in a Nonaqueous Medium." Journal of Physical Chemistry C 123, 15 (April 2019): 9713-9720 © 2019 American Chemical Society

As Published: http://dx.doi.org/10.1021/ACS.JPCC.9B00669

Publisher: American Chemical Society (ACS)

Persistent URL: https://hdl.handle.net/1721.1/124016

Version: Author's final manuscript: final author's manuscript post peer review, without publisher's formatting or copy editing

Nature of the First Electron Transfer in Electrochemical Ammonia Activation in a Non-Aqueous Medium

Zachary J Schiffer[1], Nikifar Lazouski[1], Nathan Corbin[1], Karthish Manthiram[1,*]

[1]Department of Chemical Engineering, Massachusetts Institute of Technology, Cambridge, MA 02139, USA

[*]Corresponding Author: 617-715-5740, karthish@mit.edu

Abstract

Decreasing costs of renewable sources of electricity will increase the viability of electrochemical processes in chemical manufacturing. To this end, improved understanding of electrochemical N-H bond activation is essential to develop electrochemical routes for nitrogen-containing chemicals. In this work, we investigate electrochemical ammonia activation in acetonitrile, a prototypical non-aqueous solvent for electro-organic syntheses. Non-aqueous environments are desirable for electro-organic syntheses due to large electrochemical stability windows and high solubility for organic products. We find that ammonia oxidation in acetonitrile proceeds through an outer-sphere mechanism involving an initial electron transfer as the rate-determining step, likely producing an ammonia radical cation. Density functional theory calculations explain a low transfer coefficient and suggest possible subsequent reaction steps. Structural factors involved in lowering of the transfer coefficient provide insights that are applicable to wider range of small-molecule activation chemistries.

Introduction

Increased grid penetration of renewable energy sources and improved electrical storage options are creating new opportunities for the electrification of the chemical industry. This electrification allows for the replacement of traditionally carbon-intensive chemical processes with systems that take advantage of the available renewable electricity sources to reduce carbon footprints.[1] Ammonia has one of the largest global production rates by volume; it is the key nitrogen-containing feedstock used to introduce nitrogen functionality into a wide range of chemical products, including nitrogen-containing polymers such as nylon and biochemicals such as amino acids.[2] Syntheses for these compounds generally utilize ammonia in thermochemical reactions, relying on temperature and pressure as driving forces. We are interested in developing the electrochemical analogue of these oxidation reactions, which will ideally occur at more mild conditions, increasing modularity and potentially decreasing unit costs. Electrochemical oxidation of ammonia in an aqueous environment has been extensively studied for fuel cell applications;[3,4] for electro-organic synthesis, the narrow electrochemical stability window and limited solubility of many organic molecules make water a less-than-ideal solvent. Non-aqueous electrochemical ammonia oxidation removes these constraints, and previous work has suggested that ammonia can be oxidized to nitrogen in a non-aqueous environment.[5–9]

Electro-organic amination has been previously studied, providing understanding of the mechanism and products from oxidation of various amines.[10–16] From these studies, a general consensus has emerged that oxidation of an amine first removes an electron to form a nitrogen radical cation in the rate determining step. For amines which bear an α-hydrogen, deprotonation can occur, leading to a more stable carbon radical.[15]

Alternatively, bond cleavage between the nitrogen and neighboring carbon can produce a nitrogen radical and carbocation that will further react.[11,17] Depending on the amine and the reaction conditions, bond cleavage and recombination of intermediates can result in various products.[11] While ammonia oxidation has been peripherally studied and observed to result in nitrogen gas, previous research has not focused on the mechanism of electrochemical ammonia oxidation in a non-aqueous environment.[5,11] Understanding the mechanism and intermediates involved in ammonia oxidation is a key step toward the usage of ammonia in electro-organic synthesis reactions to form products with carbon-nitrogen bonds.

Here, we show that the mechanism of electrochemical ammonia oxidation in non-aqueous media is analogous to that of amines, with some key differences intrinsic to ammonia that differentiate it from amine oxidation. The mechanisms are similar in that both ammonia oxidation and electrochemical amine oxidation proceed through an initial rate-determining electron transfer, and both mechanisms are outer-sphere. The key differences include the low transfer coefficient observed for ammonia oxidation and the fact that the ammonia radical formed from the initial electron transfer cannot be stabilized through breaking of a C-N bond or C-H bond at the α position; the nitrogen-centered radical must react with a nearby molecule. We further investigate the rate-determining step (RDS) with density functional theory (DFT) calculations that help explain the low transfer coefficient and give thermodynamic context to the rate-determining step.

Methods

Ammonia oxidation experiments were run in a two-compartment cell separated by a Celgard polypropylene separator, (**Figure S1**) with reaction conditions chosen to be similar to previous non-aqueous oxidation of ammonia[5] and primary amines.[11] The electrolyte was anhydrous acetonitrile with tetrabutylammonium tetrafluoroborate (Bu_4NBF_4) as a supporting salt; the electrolyte was saturated with ammonia gas by bubbling through the electrolyte prior to use in electrochemical experiments. The working electrode (anode) was a polished, planar glassy-carbon planar electrode, and the counter electrode (cathode) was a platinum foil. A leak-free Ag/AgCl reference electrode was used as a pseudo-reference. Calibration of the pseudo-reference was performed using ferrocene (**Figure S2**).

DFT calculations were performed using Gaussian 16 using the B3LYP functional and a 6-31++G** basis set. Reorganization energies were calculated by following the procedure previously reported in the literature and are further detailed in the Supplemental Experimental Procedures.[18] Solvation free energies were calculated using the C-PCM[19,20] model with Bondi radii.[21]

Results

Confirmation of Ammonia Oxidation

In this work, we explore electrochemical ammonia oxidation at a glassy-carbon working electrode in anhydrous acetonitrile with tetrabutylammonium tetrafluoroborate (Bu_4NBF_4) as supporting electrolyte (see Experimental Procedures). Verifying that oxidation currents arise from ammonia oxidation as opposed to solvent oxidation is essential before we can draw any mechanistic conclusions. Cyclic voltammetry (CV) of both an ammonia saturated electrolyte and an electrolyte without any ammonia demonstrates a significant increase in Faradaic current in the presence of ammonia (**Figure 1**). To rule out the possibility that there is an electrochemical reaction involving acetonitrile oxidation in the presence of ammonia, we conducted the same experiment with and without ammonia using tetrahydrofuran as the solvent and observed similar results (**Figure S3**). Furthermore, gas chromatography (GC) of the reactor effluent reveals that the only detectable gaseous product is nitrogen gas, an expected product of ammonia oxidation (**Figure S4b**). The calculated Faradaic efficiency (FE) for nitrogen production is 70 ± 14%. While this FE is below unity, meaning Faradaic current could be going to products other than nitrogen, the chromatographic results indicate that nitrogen is the major product from the ammonia oxidation. In this work, we will use the total current to represent the rate of electrochemical ammonia oxidation since the current that does not go to dinitrogen gas will not affect our conclusions (see Supplemental Experimental Procedures for further discussion). These conclusions are in agreement with previous ammonia and amine

oxidation studies, including those which used Differential Electrochemical Mass Spectrometry (DEMS), which indicate that N_2 is the sole product.[5,11]

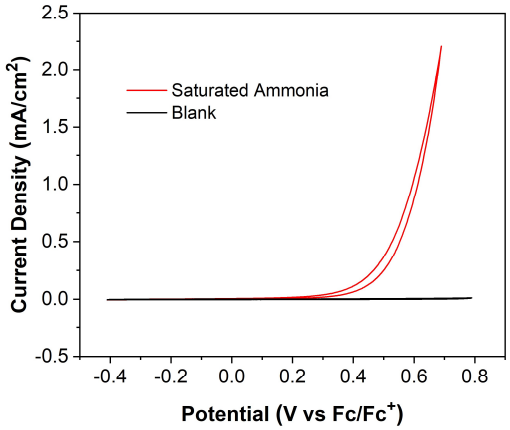

Figure 1. Evidence that current is from ammonia and not oxidation of the acetonitrile solvent. Electrolytes are anhydrous acetonitrile with 0.2 M Bu_4NBF_4 saturated with ammonia. Nitrogen quantification data at various currents were used to obtain the average N_2 FE of 70 ± 14% (see **Figure S4** for details on gas chromatograph calculations). Ammonia oxidation also occurs in THF (**Figure S3**).

Rate Law Determination

By varying their concentration, we determined the reaction rate dependence on four relevant species: ammonia, water, hydroxide ions, and protons (**Figure 2**). When the logarithm of the current is plotted against the logarithm of species concentration, the rate of ammonia oxidation is first-order in ammonia and zeroth-order in all other species, leading to the following rate law:

$$r_{NH_3} \propto [NH_3] \quad (1)$$

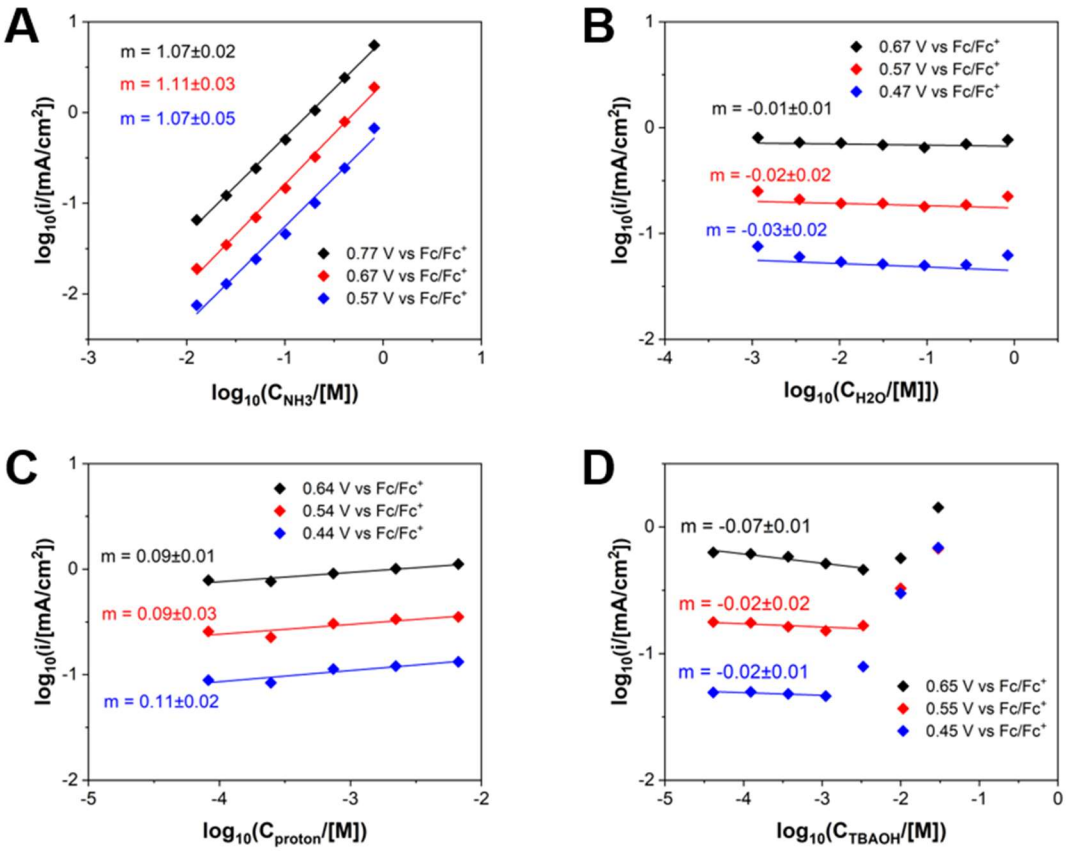

Figure 2. The ammonia oxidation reaction is first order in ammonia and zeroth-order in other species at relevant conditions. The current as a function of concentration at three different potentials is determined for ammonia (A), water (B), protons (C), and hydroxide ions (D). These experiments were run in anhydrous acetonitrile with 0.2 M Bu_4NBF_4 as supporting electrolyte.

The order dependence of current on hydroxide concentration becomes positive at high hydroxide concentrations due to hydroxide oxidation since a similar rise in current at high hydroxide concentrations is still observed in the absence of ammonia (**Figure S5**). We cannot explore the region of very high proton concentration (> ~0.01 M) because ammonium salts are not very soluble in acetonitrile, and high concentrations lead to the ammonium salt precipitating out of solution.

Outer-Sphere Mechanism

In aqueous environments, ammonia oxidation proceeds via an inner-sphere mechanism, adsorbing on metals like iridium and platinum to react.[22,23] However, *amine* oxidation in a non-aqueous environment is known to follow an outer-sphere mechanism.[15,16] We compared the reaction rate for ammonia oxidation on glassy carbon to that on platinum. The Tafel slope on glassy carbon is 183 ± 6 mV/dec and the Tafel slope on platinum is 192 ± 3 mV/dec (**Figure 3**). These values are the same to within error, indicating that the reaction has the same rate-determining electron transfer step for both mechanisms. Additionally, the magnitudes of the current responses are similar (within a factor of two). Because ammonia exhibits similar reaction rates on platinum and glassy carbon, it is unlikely that the nature of a surface catalytic site is responsible for dictating oxidation activity. Thus, the oxidation of ammonia likely proceeds through an outer-sphere mechanism.[24,25]

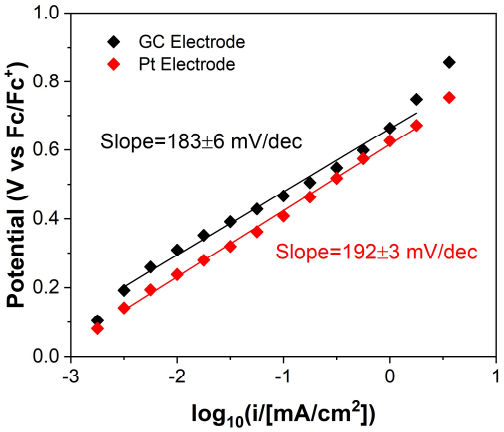

Figure 3. Comparison of ammonia oxidation on platinum and glassy carbon via Tafel analysis. The Tafel slopes are nearly identical and the current responses are sufficiently similar that the reaction is likely outer-sphere and independent of electrode material. Further discussion of the Tafel regime and the curvature is given in **Figure S6**.

Ideally, comparison of rates at a wider range of electrode materials would further prove that the mechanism is outer-sphere. However, many metals oxidize or form passivating layers under these conditions, making them unsuitable for comparison. The difference in reaction rates between platinum and glassy carbon may be due to slight surface variations that affect the reaction plane distance relative to the electrode surface. Marcus theory predicts that an outer-sphere reaction is independent of the electrode identity in the case of an adiabatic electron transfer, but in the case of a non-adiabatic electron transfer, a thin surface film or a passivating layer can cause significant variations in the intrinsic rate constant, leading to differences in activity on various metal surfaces.[26]

In studies of amine oxidation in non-aqueous electrolytes, the first electron transfer has been determined to be the rate-determining step (RDS).[11,15,16,27] If we assume that the first electron transfer is rate-limiting, we could determine the corresponding transfer coefficient. The Tafel slope at standard conditions is related to the transfer coefficient as:[28]

$$m_{Tafel} = \frac{59\frac{mV}{dec}}{\alpha} = \frac{59\frac{mV}{dec}}{n+\beta q} \quad (2)$$

Here, *n* is the number of electron transfers before the RDS, *q* is the number of electrons transferred during the RDS, *α* is the transfer coefficient, and *β* is the symmetry factor. If the first, single electron transfer is rate limiting, then $n = 0$ and $q = 1$, resulting in $\alpha = \beta$. Normally, when $\beta = \frac{1}{2}$, the Tafel slope for a first-electron-transfer RDS is 120 mV/dec. However, higher Tafel slopes are possible with smaller values of *β* and the corresponding value of α. In this case, the high Tafel slope on glassy carbon (183 ± 6 mV/dec) indicates a transfer coefficient of 0.32 ± 0.01. The rationale behind this low transfer coefficient is

explored below, and it is a unique feature for ammonia oxidation in non-aqueous solvents that is not observed for amine oxidation for which the transfer coefficients are typically near 0.5.[15]

Electron Transfer vs. Concerted Proton-Electron Transfer

Although the Tafel slope shows that the RDS is an initial electron transfer, it does not indicate whether a proton is lost simultaneously in a concerted proton-electron transfer (CPET). Accordingly, two possible reactions could serve as the RDS: an electron transfer (ET) to produce an ammonia radical cation (ET, Equation 3) or a concerted proton-electron transfer to produce a neutral amino radical (CPET, Equation 4).

$$NH_3 \rightarrow NH_3^{\cdot+} + e^- \quad (3)$$

$$NH_3 \rightarrow NH_2^{\cdot} + e^- + H^+ \quad (4)$$

A kinetic isotope experiment can help distinguish between the two possibilities. The current response from deuterated ammonia (ND_3) is very similar to regular ammonia. A linear potential sweep reveals that the kinetic isotope effect (KIE, or ratio of the current with NH_3 to ND_3), is 1.3 ± 0.1. Visually, the linear sweeps look almost identical (**Figure 4**). This small KIE could be due to factors peripheral to the molecular mechanism, such as small shifts in the equilibrium potential or exchange current density. However, a lack of KIE, although generally a good test of whether a proton transfer is involved, is not a guarantee that a CPET process does not occur; unit KIEs can lead to false negatives.[29]

To further support the ET mechanism, we can follow a simple thought experiment exploring the fate of the proton in a supposed CPET mechanism. We assume that the

ammonia would act as the proton acceptor in a hypothetical CPET because ammonia is present at high concentrations (0.8 ± 0.1 M, **Figure S7**) and is significantly more basic than any other molecule in the electrolyte. Because ammonia is likely the proton acceptor, a CPET mechanism would be more accurately written as second-order in ammonia (Equation 5).

$$2NH_3 \rightarrow NH_2^{\cdot} + e^- + NH_4^+ \quad (5)$$

However, from the previous order dependence studies, we know that the ammonia order dependence is first-order, not second-order (**Figure 2a**). Our DFT calculations suggest that Equation 3 has a standard state equilibrium potential of 1.77 V vs the Computational Hydrogen Electrode (CHE), and Equation 4 has standard potential of 2.09 V vs CHE (**Table S5**). Equation 5, as suspected, is more thermodynamically favorable, having a standard state potential of 1.11 V vs CHE. Our thought experiment following the proton from a CPET thus results in either an acetonitrile-solvated proton (Equation 4), a possibility that is thermodynamically unfavorable, or a second-order reaction with respect to ammonia (Equation 5), an experimentally disproven mechanism. Thus, we can say with reasonable confidence that the RDS involves an ET and not a CPET.

As mentioned previously, the RDS for electrochemical oxidation of amines in non-aqueous solvents is the initial electron transfer, and previous studies have determined that this initial electron transfer does not involve a concerted proton transfer, matching our findings for the RDS of ammonia oxidation.[10,15]

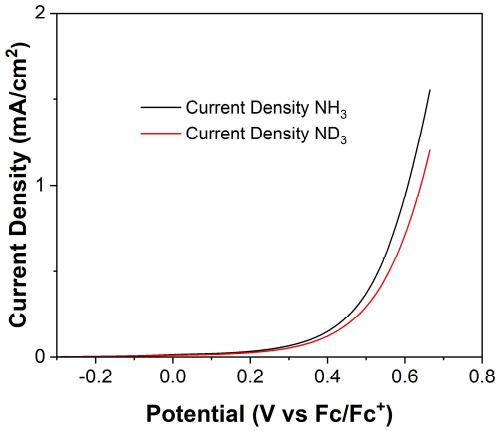

Figure 4. Determination that the RDS is an ET and not CPET through a KIE test. The current response to a linear potential sweep shows a KIE of 1.3 ± 0.1, indicating that the mechanism is likely not CPET. Electrolyte was anhydrous acetonitrile with 0.2 M Bu_4NBF_4 and scan rate was 5 mV/s.

Discussion

Overall, the electrochemical oxidation of ammonia can be well-understood from our experimental results—the only reactant is ammonia, the reaction is outer-sphere, and the RDS is an initial removal of an electron. One remaining, unexplained phenomenon is the transfer coefficient ($\alpha = 0.32 \pm 0.01$) being significantly lower than 0.5. To understand why the transfer coefficient is low, we can draw on Marcus theory for outer-sphere electron transfers.

Reorganization energies and transfer coefficients

Marcus theory gives an expression for the activation energy and the transfer coefficient:[28]

$$E_a = E_{a,0}\left(\frac{F(\phi-\phi_0)}{4E_{a,0}} - 1\right)^2 \tag{6a}$$

$$E_a = \frac{\lambda}{4}\left(\frac{F(\phi-\phi_0)}{\lambda} - 1\right)^2 = \frac{\lambda}{4} + \frac{F^2(\phi-\phi_0)^2}{4\lambda} - \frac{F(\phi-\phi_0)}{2} \tag{6b}$$

$$\alpha = -\frac{1}{F}\frac{dE_a}{d\phi} = -\frac{1}{2}\left(\frac{F(\phi-\phi_0)}{\lambda} - 1\right) \quad (6c)$$

In these equations, λ is the solvent reorganization energy, $E_{a,0}$ is the activation energy of the reaction at zero applied potential, ϕ is the applied potential, ϕ_0 is the equilibrium potential of the reaction, and F is Faraday's constant. The activation energy (Equation 6a) can be expressed in terms of the reorganization energy using the relation $E_{a,0} = \frac{\lambda}{4}$ (Equation 6b).[28] Additionally, because the rate of reaction obeys an Arrhenius relationship, a potential $\phi > \phi_0$ (for an oxidation reaction) must be applied to lower the activation energy and increase the current. The effect of a large reorganization energy (λ) on the current is twofold. First, as the reorganization energy increases, higher overpotentials ($\phi - \phi_0$) must be applied to lower the activation energy (Equation 6b, **Figure 5a**). Second, when these high overpotentials are applied, the transfer coefficient decreases (Equation 6c). In general, the change in transfer coefficient with increasing potential is not significant if relatively small overpotentials (~100 mV) can drive the reaction, resulting in a transfer coefficient near 0.5. However, when the reorganization energy increases significantly and high overpotentials are required to compensate and lower the activation energy, the measured transfer coefficient will decrease significantly (**Figure 5b**). This argument can be seen by combining Equations 6b and 6c to show find that $\alpha = \sqrt{\frac{E_a}{\lambda}}$. Thus, for a fixed activation energy and therefore a fixed current, as the reorganization energy increases, the transfer coefficient decreases.

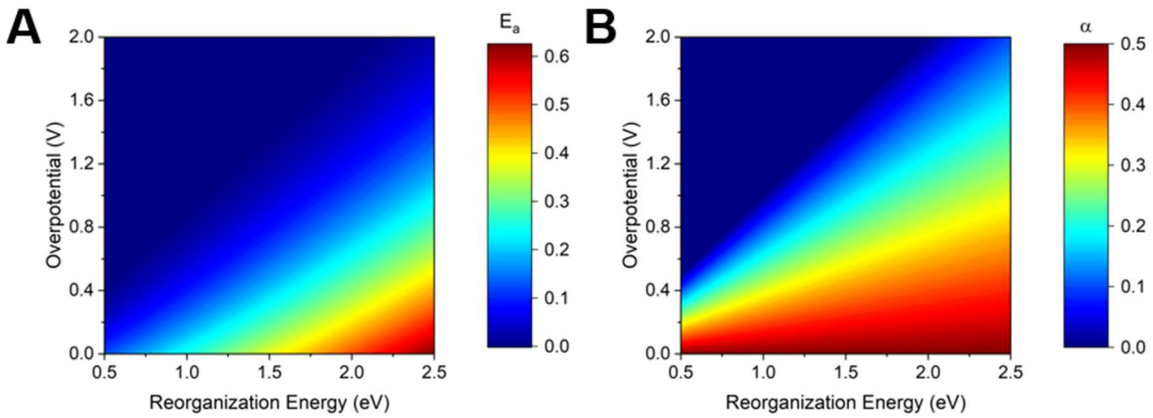

Figure 5. Demonstration of how large reorganization energies lead to high overpotentials and low transfer coefficients. According to Marcus kinetics, the activation energy (A) and transfer coefficient (B) are functions of reorganization energy and overpotential. As the reorganization energy increases, larger overpotentials are necessary to keep the activation energy small, resulting in lower transfer coefficients.

Essentially, large reorganization energies combined with Marcus kinetics can lead to low transfer coefficients because higher potentials are needed to lower the activation energy (**Figure 5**). This effect has been observed in the context of dissociative electron transfer, where a bond is broken at the same time as the electron transfers, and the intrinsic activation energy can be described by $E_{a,0} = \frac{\lambda + BDE}{4}$, which is equivalent to an increase in the reorganization energy, where BDE is the bond dissociation energy.[30,31]

Calculation of Reorganization Energy for Ammonia Oxidation

Finding the reorganization energy of ammonia oxidation experimentally requires careful measurements of the reaction rate at various temperatures, from which the activation energy can be determined, and such measurements are beyond the scope of this work. However, we may compute the reorganization energy for ammonia oxidation. Theoretical

reorganization energies are calculated using DFT according to the method of Ghosh et al. by calculating the electronic internal reorganization energy (λ_i) and the solvent reorganization energy (λ_s). λ_s is calculated by assuming that the molecule is a point charge in a spherical cavity of continuum solvent (Supplemental Experimental Procedures).[18] The total reorganization energy is then the sum of the internal and solvent reorganization energies. This method has been found to be accurate to within 0.1-0.2 eV.[18] Through this method, the reorganization energy for ammonia oxidation (Equation 3) was calculated to be 1.94 eV. This value is significantly larger than many experimentally determined reorganization energies for common outer-sphere reactions,[18,32,33] such as that of ferrocyanide oxidation in water ($\lambda = 0.99\ eV$),[33] and explains the low transfer coefficient observed in the ammonia oxidation reaction (**Figure 5b**).

The reason why ammonia oxidation has such a large reorganization energy is two-fold. First, ammonia has a large internal reorganization energy (0.45 eV) because there is a significant geometry change associated with the oxidation from trigonal pyramidal ammonia to a trigonal planar cation radical (**Figure S10**). This value is the average of the energy differences associated with the geometry change in both the oxidized and reduced electronic states (further details in Supplemental Experimental Details), and is larger than the known umbrella inversion barrier for ammonia (0.25 eV)[34] due to the larger calculated energy difference associated with a geometry change of the ammonia radical cation. Second, ammonia is a small molecule, and the removal of an electron creates a change in charge independent of molecule size. Since ammonia is so small, the surface charge density is large, requiring significant rearrangement of the solvent to compensate and

leading to a large solvent reorganization energy. These two factors combine to result in an unusually high reorganization energy for ammonia oxidation and an apparent low transfer coefficient. While Marcus theory can explain the apparent low transfer coefficient in this system, other factors such as the electric double layer can also influence the transfer coefficient. Although the double layer can theoretically cause significant deviations in the transfer coefficient, these deviations are expected to be smaller in the absence of surface-adsorption,[35] as is the case for the outer-sphere electron transfer reaction studied here.

Overall Reaction Mechanism

Since the rate-determining step of the ammonia oxidation mechanism is the first electron transfer, our experiments do not determine the mechanism after the RDS. DFT calculations reveal the thermodynamics of possible subsequent steps (**Figure 6**), an exercise that helps guide future experiments where we hope to intercept intermediates to generate other nitrogen-containing products. We constructed this thermodynamic diagram on the basis of two ammonia molecules so that a second ammonia molecule may act as a proton acceptor and to facilitate understanding of later steps in which these molecules may couple together.

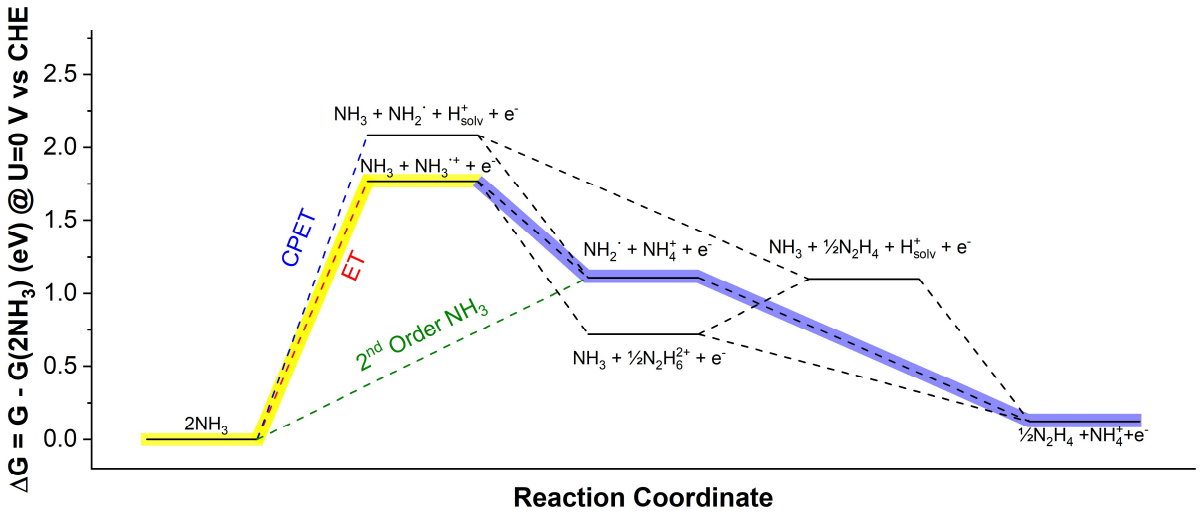

Figure 6. DFT-calculated free energies of potential intermediates and possible mechanistic steps involved in the oxidation of ammonia. Actual kinetics and deviation from standard state concentrations cause the experimentally determined RDS (yellow path) and postulated next steps (blue path) to deviate from the path of strictly lowest energy intermediates. Raw data and calculation details can be found in **Tables S2, S3,** and **S4**. We have experimentally determined that the RDS follows the yellow-highlighted path (ET).

The DFT calculations show that after the initial ET RDS (experimentally supported), the ammonia radical cation can couple with another radical to form a protonated hydrazine or can deprotonate with another ammonia molecule to form a neutral amino radical. Due to the relatively high concentration of ammonia (0.8 ± 0.1 M) and its pK_a in acetonitrile (16.5),[36] as well as the relatively low concentrations of the radical cation because of its high reactivity,[37] deprotonation will likely be the kinetically favored next step, resulting in an amino radical. In addition to our DFT calculations showing the thermodynamic favorability of the amino radical, experiments have found that the pK_a of the ammonia cation radical in water (pK_a = 3-7) is significantly lower than the pK_a of the ammonium ion (pK_a = 9.3),[38,39] further supporting the idea that the amino radical is

present when the solution pK_a is dictated by ammonia. Thermodynamically, the amino radical then likely recombines with another amino radical to form hydrazine, which further oxidizes to nitrogen gas, a process known to occur with fast kinetics in aqueous environments.[40,41] Primary amine radicals have a lifetime of <0.2 ms, and ammonia and amino radicals would be expected to live for even less time because they are less stabilized and are known to couple at very fast rates;[15,37] this instability makes their direct observation difficult. While we looked for evidence of hydrazine as an intermediate, due to hydrazine's significantly lower oxidation potential than ammonia (~1 V lower, **Figure S8**), any hydrazine produced would be rapidly oxidized and difficult to detect. While the exact mechanistic steps connecting an ammonia radical cation to the final product are beyond the scope of this work, previous research has found evidence that ammonia radicals generated via other methods, such as irradiation of cobalt hexamine (III) and pulse radiolysis in water, react to become nitrogen gas.[40,42–45]

The thermodynamic equilibrium potential for ammonia oxidation in an acetonitrile system with a buffer of known pK_a has been previously calculated;[36] our system is not buffered, making the standard state thermodynamic equilibrium potential for electrochemical conversion of ammonia to nitrogen difficult to calculate. Additionally, because the oxidation of ammonia is irreversible, determining the thermodynamic equilibrium potential experimentally is difficult. Although we do not know the exact equilibrium potential, the DFT energy landscape indicates that we are likely operating at a high overpotential relative to the thermodynamic potential of ammonia oxidation to nitrogen gas. While this high overpotential would make an ammonia fuel cell impractical and energy inefficient, it does not preclude the use of non-aqueous, outer-sphere

ammonia oxidation for electro-organic syntheses, since valuable products and facile synthetic routes can offset the economic penalties from energy losses due to large overpotentials.

Conclusion

In this work, we show that electrochemical ammonia oxidation in acetonitrile occurs via an outer-sphere mechanism in which the initial electron transfer is the rate-determining step, likely producing an ammonia radical cation. This reaction depends only on the concentration of ammonia in solution and produces nitrogen gas in the potential windows explored. DFT calculations suggest that after the initial electron transfer, the radical deprotonates and combines with another radical to form hydrazine before eventually becoming nitrogen gas. DFT calculations also explain why the apparent transfer coefficient for ammonia oxidation is so much lower than the expected value of one-half. Overall, our mechanistic understanding of N-H bond breaking provides foundational knowledge for future efforts aimed at using ammonia as an electrochemical reactant in the synthesis of valuable nitrogen-containing organic compounds

Author Contributions

All authors contributed to the preparation of this manuscript and approved the final version of the manuscript.

Supporting Information

The following files are available free of charge.

Supporting Information (PDF). In-depth materials & methods; discussions of system calibration, nitrogen and ammonia quantification, additional experimental tests, and computational details.

Acknowledgements

Z.J.S., N.C., and N.L. gratefully acknowledge the National Science Foundation Graduate Research Fellowships Program. We also acknowledge the support of the MIT Energy Initiative Seed Fund. This work used the Extreme Science and Engineering Discovery Environment (XSEDE), which is supported by National Science Foundation grant number ACI-1548562. In particular, this work used the Extreme Science and Engineering Discovery Environment (XSEDE) Comet SDSC (TG-CHE180048). We are also grateful for advice and proofreading from Kindle Williams and Deng-Tao Yang.

References

(1) Schiffer, Z. J.; Manthiram, K. Electrification and Decarbonization of the Chemical Industry. *Joule* **2017**, *1* (1), 10–14.

(2) IEA; ICCA; DECHEMA. *Technology Roadmap: Energy and GHG Reductions in the Chemical Industry via Catalytic Processes*; 2013.

(3) Katsounaros, I.; Figueiredo, M. C.; Calle-Vallejo, F.; Li, H.; Gewirth, A. A.; Markovic, N. M.; Koper, M. T. M. On the Mechanism of the Electrochemical Conversion of Ammonia to Dinitrogen on Pt(1 0 0) in Alkaline Environment. *J. Catal.* **2018**, *359*, 82–91.

(4) Bunce, N. J.; Bejan, D. Mechanism of Electrochemical Oxidation of Ammonia.

Electrochim. Acta **2011**, *56* (24), 8085–8093.

(5) Peng, W.; Xiao, L.; Huang, B.; Zhuang, L.; Lu, J. Inhibition Effect of Surface Oxygenated Species on Ammonia Oxidation Reaction. *J. Phys. Chem. C* **2011**, *115* (46), 23050–23056.

(6) Ji, X.; Silvester, D. S.; Aldous, L.; Hardacre, C.; Compton, R. G. Mechanistic Studies of the Electro-Oxidation Pathway of Ammonia in Several Room-Temperature Ionic Liquids. *J. Phys. Chem. C* **2007**, *111*, 9562–9572.

(7) Ji, X.; Banks, C. E.; Silvester, D. S.; Aldous, L.; Hardacre, C.; Compton, R. G. Electrochemical Ammonia Gas Sensing in Nonaqueous Systems: A Comparison of Propylene Carbonate with Room Temperature Ionic Liquids. *Electroanalysis* **2007**, *19* (21), 2194–2201.

(8) Buzzeo, M. C.; Giovanelli, D.; Lawrence, N. S.; Hardacre, C.; Seddon, K. R.; Compton, R. G. Elucidation of the Electrochemical Oxidation Pathway of Ammonia in Dimethylformamide and the Room Temperature Ionic Liquid, 1-Ethyl-3-Methylimidazolium Bis(Triflouromethylsulfonyl)Imide. *Electroanalysis* **2004**, *16* (11), 888–896.

(9) Ji, X.; Banks, C. E.; Compton, R. G. The Direct Electrochemical Oxidation of Ammonia in Propylene Carbonate: A Generic Approach to Amperometric Gas Sensors. *Electroanalysis* **2006**, *18* (5), 449–455.

(10) Chow, Y. L.; Nelsen, S. F.; Rosenblatt, D. H. Nonaromatic Aminium Radicals. *Chem. Rev.* **1978**, *78* (3), 243–274.

(11) Barnes, K. K.; Mann, C. K. Electrochemical Oxidation of Primary Aliphatic Amines. *J. Org. Chem.* **1967**, *32* (5), 1474–1479.

(12) Mann, C. K. Cyclic Stationary Electrode Voltammetry of Some Aliphatic Amines. *Anal. Chem.* **1964**, *36* (13), 2424–2426.

(13) O'Donnell, J. F.; Mann, C. K. Controlled-Potential Oxidation of Aliphatic Amides. *Electroanal. Chem. Interfacial Electrochem.* **1967**, *13*, 157–162.

(14) Smith, P. J.; Mann, C. K. Electrochemical Dealkylation of Aliphatic Amines. *J. Org. Chem.* **1969**, *34* (6), 1821–1826.

(15) Adenier, A.; Chehimi, M. M.; Gallardo, I.; Pinson, J.; Vilà, N. Electrochemical Oxidation of Aliphatic Amines and Their Attachment to Carbon and Metal Surfaces. *Langmuir* **2004**, *20* (19), 8243–8253.

(16) Gallardo, I.; Pinson, J.; Vilà, N. Spontaneous Attachment of Amines to Carbon and Metallic Surfaces. *J. Phys. Chem. B* **2006**, *110* (39), 19521–19529.

(17) Blackham, A. U.; Kwak, S.; Palmer, J. L. Electrochemical Oxidation of Tert-Butylamine to 2,2'-Aziosobutane. *J. Electrochem. Soc.* **1975**, 1081–1082.

(18) Ghosh, S.; Horvath, S.; Soudackov, A. V.; Hammes-Schiffer, S. Electrochemical Solvent Reorganization Energies in the Framework of the Polarizable Continuum Model. *J. Chem. Theory Comput.* **2014**, *10* (5), 2091–2102.

(19) Cossi, M.; Rega, N.; Scalmani, G.; Barone, V.; Chimica, D.; Ii, F.; Angelo, C. M. S. Energies, Structures, and Electronic Properties of Molecules in Solution with the C-PCM Solvation Model. **2003**, *24* (6), 669–681.

(20) Barone, V.; Cossi, M. Quantum Calculation of Molecular Energies and Energy Gradients in Solution by a Conductor Solvent Model. *J. Phys. Chem. A* **1998**, *102* (11), 1995–2001.

(21) Bondi, A. Van Der Waals Volumes and Radii. *J. Phys. Chem.* **1964**, *68* (3), 441–

451.

(22) De Vooys, A. C. A.; Mrozek, M. F.; Koper, M. T. M.; Van Santen, R. A.; Van Veen, J. A. R.; Weaver, M. J. The Nature of Chemisorbates Formed from Ammonia on Gold and Palladium Electrodes as Discerned from Surface-Enhanced Raman Spectroscopy. *Electrochem. commun.* **2001**, *3* (6), 293–298.

(23) De Vooys, A. C. A.; Koper, M. T. M.; Van Santen, R. A.; Van Veen, J. A. R. The Role of Adsorbates in the Electrochemical Oxidation of Ammonia on Noble and Transition Metal Electrodes. *J. Electroanal. Chem.* **2001**, *506* (2), 127–137.

(24) Kravtsov, V. I. Outer and Inner Sphere Mechanisms of Electrochemical Steps of the Metal Complexes Electrode Reactions. *J. Electroanal. Chem.* **1976**, *69*, 125–131.

(25) Torres, L. M.; Gil, A. F.; Galicia, L.; Gonzalez, I. Understanding the Difference between Inner- and Outer-Sphere Mechanisms. *J. Chem. Educ.* **1996**, *73* (8), 808–810.

(26) Schmickler, W.; Santos, E. Theoretical Considerations of Electron-Transfer Reactions BT - Interfacial Electrochemistry; Schmickler, W., Santos, E., Eds.; Springer Berlin Heidelberg: Berlin, Heidelberg, 2010; pp 99–115.

(27) Portis, L. C.; Klug, J. T.; Mann, C. K. Electrochemical Oxidation of Some Phenethylamines. *J. Org. Chem.* **1974**, *39* (24), 3488–3494.

(28) Bard AJ, Faulkner LR. *Electochemical Methods Fundamentals and Applications*; 2001.

(29) Huynh, M. T.; Mora, S. J.; Villalba, M.; Tejeda-Ferrari, M. E.; Liddell, P. A.; Cherry, B. R.; Teillout, A. L.; MacHan, C. W.; Kubiak, C. P.; Gust, D.; et al.

Concerted One-Electron Two-Proton Transfer Processes in Models Inspired by the Tyr-His Couple of Photosystem II. *ACS Cent. Sci.* **2017**, *3* (5), 372–380.

(30) Houmam, A. Electron Transfer Initiated Reactions: Bond Formation and Bond Dissociation. *Chem. Rev.* **2008**, *108* (7), 2180–2237.

(31) Saveant, J.-M. Electron Transfer, Bond Breaking and Bond Formation. *Adv. Phys. Org. Chem.* **2000**, *35*, 117–192.

(32) Ghosh, S.; Soudackov, A. V.; Hammes-Schiffer, S. Electrochemical Electron Transfer and Proton-Coupled Electron Transfer: Effects of Double Layer and Ionic Environment on Solvent Reorganization Energies. *J. Chem. Theory Comput.* **2016**, *12* (6), 2917–2925.

(33) Ghosh, S.; Hammes-Schiffer, S. Calculation of Electrochemical Reorganization Energies for Redox Molecules at Self-Assembled Monolayer Modified Electrodes. *J. Phys. Chem. Lett.* **2015**, *6* (1), 1–5.

(34) Swalen, J. D.; Ibers, J. A. Potential Function for the Inversion of Ammonia. *J. Chem. Phys.* **1962**, *36* (7), 1914–1918.

(35) Huang, J.; Chen, S. Interplay between Covalent and Noncovalent Interactions in Electrocatalysis. *J. Phys. Chem. C* **2018**, *122* (47), 26910–26921.

(36) Lindley, B. M.; Appel, A. M.; Krogh-Jespersen, K.; Mayer, J. M.; Miller, A. J. M. Evaluating the Thermodynamics of Electrocatalytic N2 Reduction in Acetonitrile. *ACS Energy Lett.* **2016**, *1*, 698–704.

(37) Pagsberg, P. B. Investigation of the NH2 Radical Produced by Pulse Radiolysis of Ammonia in Aqueous Solution. *RISO Rep.* **1972**, No. 256, 209–222.

(38) Hoffman, M. Z.; Olson, K. R. The NH3+ Radical in Aqueous Solution. *J. Phys.*

Chem. **1978**, *82* (24), 2631–2632.

(39) Simic, M.; Hayon, E. Intermediates Produced from the One-Electron Oxidation and Reduction of Hydroxylamines. Acid-Base Properties of the Amino, Hydroxyamino, and Methoxyamino Radicals. *J. Am. Chem. Soc.* **1971**, *93* (23), 5982–5986.

(40) Buxton, G. V; Lynch, D. A.; July, R.; August, A. Investigation of the NH2 Radical in Aqueous Solution up to 200 C by Pulse Radiolysis. *J. Chem. Soc. Faraday Transl.* **1998**, *94*, 3271–3274.

(41) Neta, P.; Huie, R. E.; Ross, A. B.; Neta, P.; Huie, R. E.; Ross, A. B. Rate Constants for Reactions of Inorganic Radicals in Aqueous Solution Rate · Constants for Reactions of Inorganic Radicals in Aqueous Solution. *J. Phys. Chem. Ref. Data* **1988**, *17*, 1027–1284.

(42) Manfrin, M. F.; Varani, G.; Moggi, L.; Balzani, V. Photochemistry of the Hexaminecobalt(III) and Tris(Ethylenediamine)Cobalt(III) Ions. *Mol. Photochem.* **1969**, *1*, 387–402.

(43) Endicott, J. F.; Hoffman, M. Z. Photoreduction of Cobalt(III) Complexes at 2537 A. *J. Am. Chem. Soc.* **1965**, *87*, 3348–3357.

(44) Neta, P.; Maruthamuthu, P.; Carton, P. M.; Fessenden, R. W. Formation and Reactivity of the Amino Radical. *J. Phys. Chem.* **1978**, *82* (17), 1875–1878.

(45) Yuzawa, H.; Mori, T.; Itoh, H.; Yoshida, H. Reaction Mechanism of Ammonia Decomposition to Nitrogen and Hydrogen over Metal Loaded Titanium Oxide Photocatalyst. *J. Phys. Chem. C* **2012**, *116*, 4126–4136.

TOC Graphic